# Modeling acoustic response of deepwater completions using spectral method

*Florian Karpfinger*, Curtin University of Technology, Andrey Bakulin, WesternGeco, Boris Gurevich, Curtin University of Technology and CSIRO Petroleum*


## SUMMARY

Deepwater production often hinges on the ability to safely complete and effectively draw down a small number of very challenging wells. Chances of success are greatly increased if surveillance tools are available to quickly diagnose downhole conditions and detect potential issues early on. Real-time completion monitoring with acoustic waves (RTCM) has great potential for diagnosing problems in sand-screened deepwater completions. RTCM utilizes tube waves to detect permeability changes and passive noises to characterize perforation flow. Interaction of a single tube wave with permeable formations in open boreholes is well explained by Biot theory of poroelasticity. However experimental studies in laboratory models of sand-screened completions reveal presence of fast and slow tube waves that behave differently. In this paper, we simulate the dispersion and attenuation of the two tube waves by examining the solutions of Biot's equations of poroelasticity in cylindrical structures using spectral method.


## INTRODUCTION

At low frequencies, wave propagation in an open borehole is dominated by tube or Stoneley wave. Waves compress the fluid column and lead to a piston-like motion. When fluid is compressed, it expands radially and pushes against the formation or casing. In the presence of permeable borehole wall, fluid movement across the interface leads to a slowdown in velocity and an increase in attenuation. These effects are well explained by Biot's theory (Biot, 1962) and form the foundation for estimating near-wellbore permeability from an open-hole acoustic logging (Winkler et al., 1989).

Sand-screened deepwater completion has a more complicated structure (Figure 1) due to multiple permeable layers. The sand screen represents an additional pipe with a very high permeability. Annulus between the casing and screen is filled with gravel sand or fluid both of which possess negligible shear modulus. Presence of two fluid-like columns in the completion gives birth to two tube waves: fast and slow. They have been observed in experiments with full-scale laboratory models of deepwater completion (Bakulin et al., 2008a, 2009). It has been suggested that, to first approximation, sand screen can be modeled as a poroelastic Biot's layer . Most basic task of RTCM is to monitor changes in the permeability of the sand screen and gravel-pack layer. Here we aim to examine the effect of sand-screen permeability on velocities and attenuation of two tube waves. Such signatures are usually derived using an analytical root-finding technique that is difficult to implement for multi-layered attenuative poroelastic structures. Spectral method is a new approach to bypass the difficulties of root-finding for fluid and elastic cylindrical structures, and was recently extended to poroelastic cylindrical structures (Karpfinger et al., 2008a,b, 2009). By directly discretizing the underlying differential equations in the radial direction, the spectral method handles with ease such complicated cylindrical structures and obtain phase velocities and attenuation of all modes as a function of frequency.

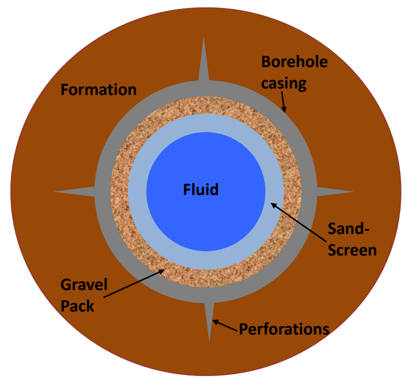


Figure 1: Deepwater completion built of various permeable layers (topview).

## SPECTRAL METHOD

*Root finding* is a direct analytical technique and hence the most natural method for analysis of the dispersion. In this technique a general solution to Helmholtz equations , expressed in terms of Bessel functions is found. Substituting the solution into the stress and displacement components yields a homogenous system of linear algebraic equations. In order to have non-trivial solutions the determinant of its matrix $M$ must be equal to zero, $\det M(\omega, k_z) = 0$. This is called the frequency equation. The roots of this equation yield the dispersion relation $\omega(k_z)$. However this method becomes difficult to implement when poroelastic effects are taken into account, as separation of different roots in the complex plane becomes challenging.

The spectral method bypasses these difficulties and solves the underlying Helmholtz equations numerically. For elastic wave propagation this was first implemented by Adamou and Craster (2004) who investigated circumferential waves in an elastic annulus. The problem is solved by numerical interpolation using spectral differentiation matrices (DMs). For axisymmetric waves in cylindrical structures with arbitrary fluid solid layers the approach was expanded by Karpfinger et al. (2008a). We have subsequently extended the approach for cylindrical, poroelastic structures (Karpfinger et al., 2008b, 2009).

## THE POROELASTIC EIGENVALUE PROBLEM

The eigenvalue problem for structures with an arbitrary number of layers can be expressed as an matrix equation in the following form

$$\tilde{L}\mathbf{\Theta} = k_z^2 Q \mathbf{\Theta} \quad . \tag{1}$$

$\tilde{L}$ is a matrix built of the differential operators of the Helmholtz equations for each layer. For lines corresponding to interfaces or the surface of a structure the differential operators of the boundary conditions are introduced. For poroelastic interfaces the relevant conditions to be considered are discussed by Deresiewicz and Skalak (1963); Gurevich and Schoenberg (1999). The boundary conditions are set equal to zero on the right hand side of eq. (1) using a diagonal unit matrix $Q$ of the same size as $\tilde{L}$. For the same components where in $\tilde{L}$ the boundary condition differential operators are introduced the value is set equal to zero in $Q$. The eigenvalues are the squared wavenumbers $k_z^2$ and $\mathbf{\Theta}$ represent the displacement potentials of the different layers. Eq. (1) is a generalized algebraic eigenvalue problem which can be solved using for example the MATLAB routine `eig`.

The phase velocities can be obtained from the real part of the wavnumbers $k_z$ as

$$v_{ph} = \frac{\omega}{\mathfrak{Re}(k_z)}. \qquad (2)$$

The corresponding attenuation $Q^{-1}$ is defined as

$$Q^{-1} = \frac{\mathfrak{Im}(k_z)}{\mathfrak{Re}(k_z)}. \qquad (3)$$

Solving this generalized eigenvalue problem (equation 1) for a range of frequencies allow the computation of the dispersion and attenuation of all modes propagating in the considered structure.

Eigenvectors corresponding to the displacement potentials $\mathbf{\Theta}$ can be used to compute the radial distribution of the displacement and stress components.

## EXPERIMENTAL OBSERVATIONS IN MODELS OF SAND-SCREENED DEEPWATER COMPLETIONS

Bakulin et al. (2009) described experiments in a full-scaled laboratory model of idealized completion. Figure 2 shows schematics as well as actual photograph of the setup. The outer pipe simulates the casing string, whereas the inner pipe represents the sand screen. The sand screen has aluminum base pipe and plastic wire wraps (Figure 2c). To simulate the impermeable or plugged sand screen, a blank pipe was used (Figure 2d). The casing was impermeable (closed perforations) and the experimental study focused on studying effects of the screen permeability on the signatures of the fast and slow tube waves.

If the sand screen is impermeable (blank pipe), then theory predicts existence of four wave modes at low frequencies, all without attenuation (Figure 3): two tube waves and two plate (extensional) waves. Two tube waves exist because completion contains two fluid columns: one inside the screen, the other in the annulus. The two plate waves are supported by the screen (inner pipe) and casing (outer pipe), respectively. If formation is added on the outside of the casing, then the casing-supported plate wave disappears, while all three other modes remain (see Figure 1).

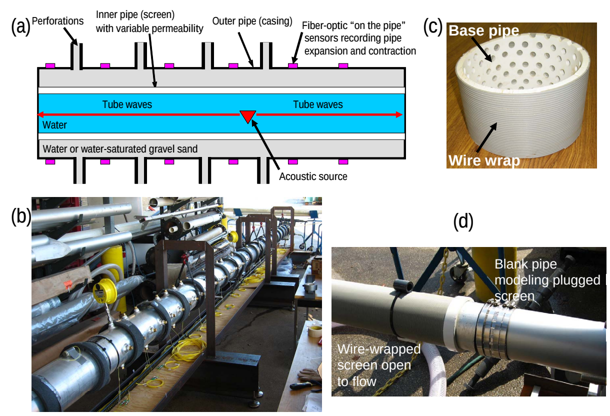


Figure 2: Sketch (a) and photograph (b) of the full-scale laboratory setup used to simulate completed horizontal well; (c) cross-section of the screen showing wire wrap and base pipe (although plastic base pipe is shown, aluminum one was actually used in the experiment); (c) wire-wrapped sand screen open to flow and blank pipe simulating plugged screen.

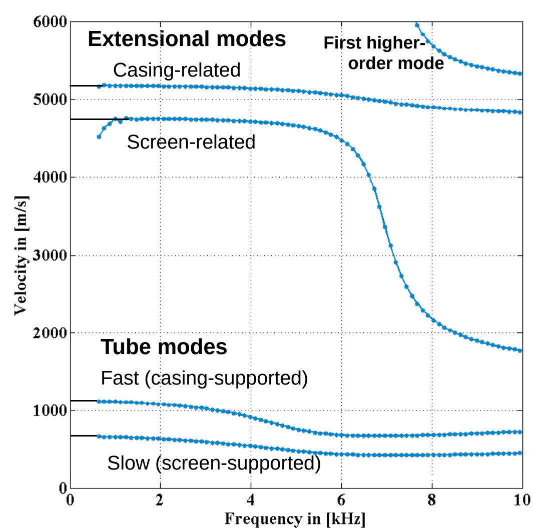


Figure 3: Dispersion curves for an idealized completion model (water-impermeable screen-water-casing-vacuum) when sand screen has vanishing permeability. Note that all modes are completely lossless. Two slowest modes represent tube waves associated with the two fluid columns whereas two fastest modes represent plate (extensional) modes in a screen and casing tubulars respectively.

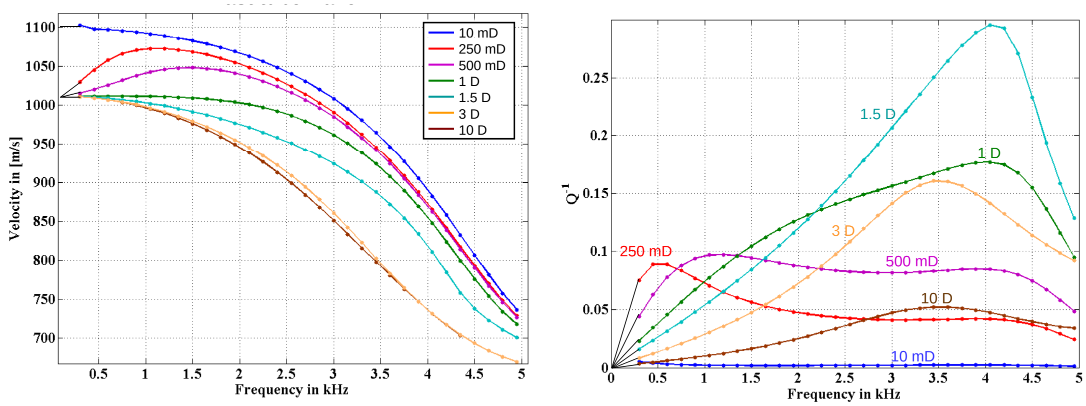


(a) (b)

Figure 4: Velocity (a) and attenuation (b) of the fast tube-wave mode as a function of screen permeability in an idealized completion model (water-permeable screen-water-casing-vacuum). Dots denote computations by spectral method, whereas thin black lines show extrapolated behavior at low frequencies where current implementation of the spectral method is numerically unstable.

## EFFECT OF SCREEN PERMEABILITY ON TUBE WAVE

Let us examine how velocities and attenuation of two tube waves depend on the screen permeability, and compare them with the behavior of these signatures for a single tube wave in case of an open borehole surrounded by infinite fluid-saturated and permeable formation (Winkler et al., 1989). In the open-hole model at low frequencies, tube-wave velocity decreases and attenuation increases with increasing formation permeability. In a completion model, we have two tube waves and their behavior is different.

Figure 4 and 5 show modeled velocity and attenuation of fast and slow tube waves as a function of screen permeability. Let us first examine the fast tube wave, which is mainly supported by the casing. In the low-permeability limit, the screen behaves as an impermeable pipe and fast tube wave experiences no loss as already shown in Figure 3. At the other extreme, when the screen is very permeable, it provides almost no resistance to the radial fluid motion across the screen and behaves like a layer of liquid. Therefore we expect to have a single (fast) tube wave supported by casing, again without a loss. From this transition we deduce that the fast tube wave is mainly supported by the casing. What would happen for intermediate permeabilities and how picture at one extreme connects to the other?

For sub-Darcy range of permeabilities, attenuation of the fast tube wave increases with increasing permeability. However this elevated attenuation peaks at about 1.5 Darcy and then decreases, returning to the state of virtually no attenuation at large permeability (Figure 4b). To a first order, the location of the attenuation maximum is controlled by screen permeability and thickness. When the screen becomes more permeable, the different rates of compression inside the two liquid columns lead to a fluid exchange across the screen. This exchange particularly intensifies for permeabilities 1.5 Darcy, where the attenuation reaches maximum.

As for the fast tube-wave velocity, it slows down progressively, with most of the changes occurring between 250 mDarcy and 3 Darcy (Figure 4a). While one normally expects velocity slowdown with the increased attenuation, it is unusual to observe that velocity continues to decrease even when attenuation starts to drop between 1.5 and 10 Darcy.

The slow tube wave demonstrates a behavior that is more similar to that of a single tube wave in an open borehole surrounded by a permeable formation. Attenuation is increasing progressively with increasing permeability (Figure 5b). While in open borehole, the tube wave always remains a propagating mode ($Q^{-1} \leq 2$, e.g. wave attenuates within more than one wavelength), in a completion the slow tube wave may become non-propagatory ($Q^{-1} > 2$ ) at a finite frequency and thus attenuates within less than a wavelength (Figure 5b). Such behavior of the slow mode can be explained using radial profiles of displacement (Bakulin et al., 2008b). It is shown that the axial displacement has opposite sign in the inner and outer fluid columns. This distinct feature makes slow tube mode analogous to a Biot's slow body wave. When the screen becomes permeable, this out of phase motion in the two columns naturally leads to an elevated fluid communication between two liquid columns. As a result, we observe rapid increase in attenuation (Figure 5b) and eventually a complete absorption of the slow mode at higher permeabilities.

In line with the increased attenuation at low frequencies, the velocity of the slow tube wave drastically decreases (Figure 5a). One important observation is that at zero frequency, the slow tube wave velocity approaches a positive value, whereas for a finite permeability it is expected to vanish at zero frequency similarly to the tube wave in an open borehole. Current implementation of the spectral method (Karpfinger et al., 2008a,b, 2009) becomes numerically unstable at very low frequencies, and therefore these conclusions are tentative and need to be verified by additional research. Interestingly, at higher frequencies, the velocity of the slow mode increases with permeability increase (Figure 5a) and may even exceed the impermeable limit. This has been also observed for a simpler model of open borehole in fluid-saturated formation (Winkler et al., 1989).

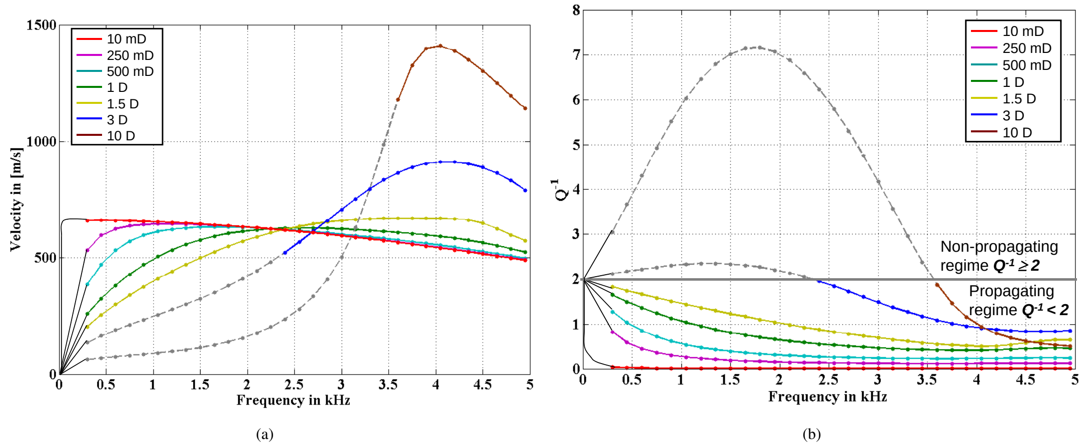


Figure 5: Velocity (a) and attenuation (b) of slow tube-wave mode as a function of screen permeability in an idealized completion model (water-permeable screen-water-casing-vacuum). Notation is the same as in Figure 3. Horizontal gray line ($Q^{-1} = 2$) separates non-propagating ( $Q^{-1} \geq 2$ ) and propagating regimes ( $Q^{-1} < 2$). In addition, curves are grayed out for frequencies where the slow mode becomes non-propagating and attenuates within less than a wavelength.

## CONCLUSIONS

Modeling with spectral method confirms strong dependence of fast and slow tube-wave signatures on the screen permeability. Therefore, acoustic surveillance system installed in a deepwater completion has a great chance to detect sand-screen plugging in real time. Sand-screen plugging is a serious problem that can create high skin factor for a well and cause a substantial decrease in production rates and thus well underperformance. However, without surveillance, it is virtually impossible to identify the source of the well underperformance, since it may be caused by other completion problems such as perforation plugging, near-wellbore permeability reduction (formation damage) or large-scale issues such as reservoir compartmentalization. Real-time completion monitoring with acoustic wave may reveal actual source of well underperfomance and thus lead to a safer and more prolific drawdown and production strategies. RTCM has the potential to revolutionize our ability to manage deepwater wells by understanding evolution of flow, drawdown and impairment in real time.

To accomplish these ambitious goals, we need to have good understanding of how acoustic signatures of interest depend on permeability of various completion layers. In this study, we concentrated on the analysis of the simplest completion model without gravel pack, and assumed that the sand screen can be modeled as a poroelastic Biot's layer. We verified that in this case the wave propagation is dominated by fast and slow tube modes supported by casing and screen, respectively. We studied the effect of screen permeability on the velocity and attenuation of fast and slow tube waves. For the slow tube-wave, velocity decreases and attenuation increases with increasing screen permeability. Such behavior is caused by escalating fluid communication between two fluid columns and can be explained by opposite signs of axial fluid displacements on different sides of the screen. In contrast, the fast tube wave experiences moderate attenuation at some characteristic frequency, which is controlled by screen permeability and thickness, whereas for small and large permeability fast tube wave remains free of losses. In the limit of high permeability, the fast tube wave transforms into a regular tube wave as if the sand screen becomes part of the surrounding liquids.

These modeling results are in a qualitative agreement with experimental observations in full-scale laboratory models of deepwater completions (Bakulin et al., 2008a,b,c, 2009). The main discrepancy is related to the behavior of the slow tube wave. Simple calculation of static screen permeability suggests values larger than 100 Darcy for which modeling predicts complete dissipation of the slow mode (Figure 5b). However experiments (Bakulin et al., 2009) reveal that slow tube waves are observed and survive even when water in the annulus is replaced by water-saturated gravel sand. Better model of sand screens is required to reconcile this discrepancy. Understanding the connection between static and "dynamic" or "acoustic" permeability for meso-scale structures such as sand screens and perforated casing is a key to such reconciliation.


## ACKNOWLEDGMENTS

We are grateful to Boris Kashtan (St. Petersburg State University) who suggested the idea of applying the spectral method to the problem at hand and Richard Craster (Imperial College) for helpful advice. We greatly appreciate discussion with David L. Johnson (SDR). Florian Karpfinger thanks Shell Int. E & P Inc. for support of his PhD project.

**EDITED REFERENCES**

Note: This reference list is a copy-edited version of the reference list submitted by the author. Reference lists for the 2009 SEG Technical Program Expanded Abstracts have been copy edited so that references provided with the online metadata for each paper will achieve a high degree of linking to cited sources that appear on the Web.

**REFERENCES**

Adamou, A. T. I., and R. V. Craster, 2004, Spectral methods for modelling guided waves in elastic media: Journal of the Acoustical Society of America, **116**, 1524–1535.

Bakulin, A., D. Alexandrov, A. Sidorov, and B. Kashtan, 2009, Acoustic waves in sand-screened deepwater completions: Comparison of experiments and modeling: Geophysics, **74**, no. 1, E45–E56.

Bakulin, A., M. Jaaskelainen, A. Sidorov, and B. Kashtan, 2008a, Downhole acoustic surveillance of deepwater wells: The Leading Edge, **27**, 518–531.

Bakulin, A., F. Karpfinger, and B. Gurevich, 2008b, Understanding acoustic response of deepwater completions: The Leading Edge, **27**, 260–267.

Bakulin, A., A. Sidorov, B. Kashtan, and M. Jaaskelainen, 2008c, Real-time completion monitoring with acoustic waves: Geophysics, **73**, no. 1, E15–E33.

Biot, M. A., 1962, Generalized theory of acoustic propagation in porous dissipative media: Journal of the Acoustical Society of America, **34**, 1254–1264.

Deresiewicz, H., and R. Skalak, 1963, On uniqueness in dynamic poroelasicity: Bulletin of Seismological Society of America., **53**, 783–788.

Gurevich, B., and M. Schoenberg, 1999, Interface conditions for Biot’s equations of poroelasticity: Journal of the Acoustical Society of America, **105**, 2585–2589.

Karpfinger, F., B. Gurevich, and A. Bakulin, 2008a, Computation of wave propagation along cylindrical structures using the spectral method: Journal of the Acoustical Society of America, **124**, 859–865.

———, 2008b, Modeling of axisymmetric wave modes in aporoelastic cylinder using spectral method: Journal of the Acoustical Society of America, **124**, EL230–EL235.

———, 2009, Poromechanics IV: personal communication.

Winkler, K. W., H.-L. Liu, and D. L. Johnson, 1989, Permeability and borehole Stoneley waves: Comparison between experiment and theory: Geophysics, **54**, 66–75.